

DIAGRAMS E_r - m_{KOH} FOR IRON AT 25–125 °C AND AT TOTAL PRESSURE OF 1–30 Bar*

Jan BALEJ^a and Jiri DIVISEK^b

^a Consultant Bureau for Chemical Engineering, Johanniterstr. 28, 86609 Donauwörth, Germany

^b Institute of Energy Process Engineering (IEV), Research Center Jülich (KFA), 52425 Jülich, Germany; e-mail: rbe056@aix.sp.kfa-juelich.de

Received January 26, 1996

Accepted June 26, 1997

Taking into consideration the water activity $a_{\text{H}_2\text{O}}$, the equilibrium pressure of water vapour $p_{\text{H}_2\text{O}}$ in or above KOH solutions of different molality (2–18 mol kg⁻¹) and temperature (0–200 °C), the relations for the quantitative evaluation of the equilibrium conditions of individual reactions in the Fe–KOH–H₂O system were derived in potential range from –0.3 to +1.8 V (RHE). With the aid of standard thermodynamic data for individual reaction components, E_r - m_{KOH} diagrams were constructed for iron at 25, 100 and 125 °C and a total pressure of 1, 10 and 30 bar (0.1, 1 and 3 MPa). Under standard conditions ($a_{\text{H}_2\text{O}} = 1.0$), Fe(OH)₂(s) may result at temperatures of up to 63.1 °C, while at higher temperatures solid magnetite, Fe₃O₄, is directly formed as the thermodynamically stable primary corrosion product. The region of existence of solid Fe(OH)₂ is influenced by the molality and temperature of KOH solutions in contact with metallic iron. For example, at 25 °C Fe(OH)₂ can only arise as the primary corrosion product in KOH solutions $m_{\text{KOH}} \leq 6.34 \text{ mol kg}^{-1}$, which cannot be concluded from the usual E_r -pH diagram after Pourbaix.

Key words: Iron oxo compounds; Iron corrosion products.

In previous works on E_r -pH diagrams for iron^{1–7} the water activity was considered to be equal to 1.0 in the pH range from –2 to +16, as usual for Pourbaix diagrams¹. This simplifying assumption deviates, particularly in highly acid or alkaline solutions, quite considerably from reality and may have led to distorted results. In order to elucidate the catalytic effect of Fe(III) substances on the anodic oxygen evolution at Ni anodes and their further behaviour under conditions of advanced water electrolysis with an intermittent operating mode appropriate calculations have been done in which the water activity and water vapour partial pressure in and over KOH solutions of various molality and temperature⁸ were taken into account. In “classical” Pourbaix diagrams potentials are related to the potential of the standard hydrogen electrode (SHE) (at pH 0). In our calculations potentials were related to more practical and experimentally easily achiev-

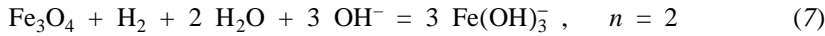
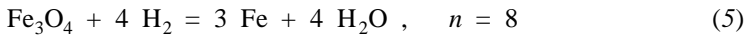
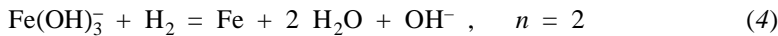
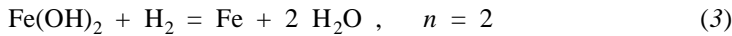
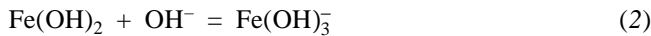
* 1 bar = 10⁵ Pa.

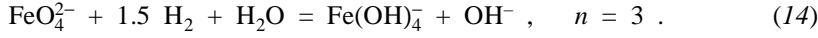
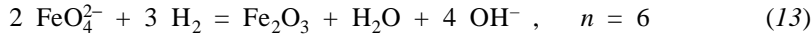
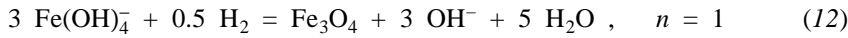
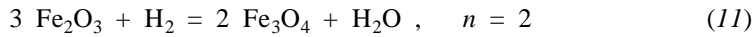
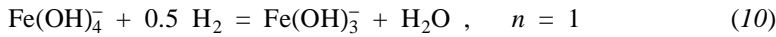
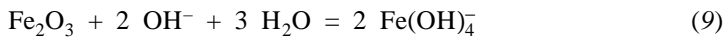
able reference hydrogen electrode (RHE) placed into experimental electrolyte solution at given temperature and total pressure. The details were already described in our previous paper⁹.

The present work deals with calculations of the equilibrium conditions of metallic iron and its oxo compounds in contact with KOH solutions in the molality range of 2–18 mol kg⁻¹ at 25–125 °C and 1–30 bar total pressure in dependence on the electrode potential range from –0.3 to +1.8 V (RHE). The results which may be of interest not only for the above given purposes but undoubtedly also for other technical as well as theoretical applications are presented in this paper.

CALCULATIONS

According to preliminary calculations, only metallic α -Fe and furthermore Fe(OH)_2 , Fe_3O_4 and $\alpha\text{-Fe}_2\text{O}_3$ were considered as solid, thermodynamically stable substances of the system under study, and Fe(OH)_3^- , Fe(OH)_4^- and FeO_4^{2-} as soluble ions. Solid FeO was not taken into account since it disproportionates spontaneously to Fe_3O_4 and Fe at temperature below 155.5 °C. Both Fe(OH)_3 and $\alpha\text{-FeOOH}$ need not be considered either, due to their dehydration to $\alpha\text{-Fe}_2\text{O}_3$ which is the only thermodynamically stable solid Fe(III) oxo compound. This conclusion is valid for standard conditions ($a_{\text{H}_2\text{O}} = 1.0$) as well as for concentrated KOH solutions with reduced water activity in the entire temperature range considered. Calculations were thus restricted to the following chemical and electrochemical cell reactions with hydrogen reference electrode placed in common solution (with n denoting the number of exchanged electrons):





The thermodynamic standard data of most reaction components at 25 °C were taken from refs^{10–14}, data for $\text{FeO}_4^{2-}(\text{aq})$ were taken from the original literature¹⁵. All used data are compiled in Table I. The coefficient of the general form of the temperature dependence of the molar heat capacity for pure substances

$$C_p^0 = a + b \cdot 10^{-3} T + c \cdot 10^{-6} T^2 + d \cdot 10^5 T^{-2} \quad (\text{J mol}^{-1} \text{ K}^{-1}) \quad (15)$$

TABLE I
Thermodynamic standard values of single Fe-substances at 25 °C

Substance	$-\Delta H_f^0, \text{ kJ mol}^{-1}$	$-\Delta G_f^0, \text{ kJ mol}^{-1}$	$S^0, \text{ J mol}^{-1} \text{ K}^{-1}$	Reference
$\alpha\text{-Fe(s)}$	0.0	0.0	27.085	10
$\text{Fe(OH)}_2(\text{s})$	574.045	491.969	87.864	11
$\alpha\text{-Fe}_2\text{O}_3(\text{s})$	825.503	743.523	87.4	11
$\text{Fe}_3\text{O}_4(\text{s})$	1 118.383	1 015.227	146.147	12
$\text{Fe(OH)}_3^-(\text{aq})$	–	614.9	299	13, 16
$\text{Fe(OH)}_4^-(\text{aq})$	–	842.2	24.5	14
$\text{Fe(OH)}_4^{2-}(\text{aq})$	481.16	322.17	37.7	15
$\text{H}_2(\text{g})$	0.0	0.0	130.684	13
$\text{H}_2\text{O}(\text{liq})$	285.830	237.129	69.91	13
$\text{OH}^-(\text{aq})$	229.994	157.244	–10.75	13

calculated from JANAF Tables¹¹ are given in Table II. Relations for mean molar heat capacity of ions, $\overline{C_p^0}|_{T_1}^T$, in the temperature range T_1 and T , where $T_1 = 298.15$ K, according to the "correspondence principle" of Criss and Cobble¹⁷ are summarized in Table III.

The calculated values of $\Delta G_{(i)}^0$ and $E_{(i)}^0$ of individual reactions in the temperature range from 25 to 125 °C are compiled in Tables IV and V, respectively.

For reaction (I), $\Delta G_{(I)}^0$ changes from slightly positive to negative with rising temperature. The value $\Delta G_{(I)}^0 = 0$ J mol⁻¹ is reached at $T_c = 336.25$ K. At this critical temperature all three solid reaction components may coexist in contact with pure water ($a_{H_2O} = 1.0$). Below this temperature $Fe(OH)_2$ remains stable and above this temperature it disproportionates spontaneously to Fe_3O_4 and Fe . This result is in agreement with the E_r -pH diagram after Silverman⁶, according to which $Fe(OH)_2$ is formed as the primary corrosion product of iron in pure water at 25 °C. Equilibrium established between metallic iron and concentrated KOH solutions may be influenced significantly because the

TABLE II
Coefficients of the Eq. (15) of individual pure substances

Substance	<i>a</i>	<i>b</i>	<i>c</i>	<i>d</i>
α -Fe(s)	23.765	5.4841	14.888	-1.457
$Fe(OH)_2$ (s)	75.092	74.777	-25.304	1.7212
α - Fe_2O_3 (s)	98.269	77.822	-	-14.853
Fe_3O_4 (s)	252.84	-226.91	296.91	-54.101
H_2 (g)	26.2164	4.3911	-0.2331	1.4327
H_2O (liq)	109.91	-189.11	273.87	2.1831

TABLE III
Relations for the average values of molar heat capacities $\overline{C_p^0}|_{T_1}^T$ of ions between $T_1 = 298.15$ K and T , according to the "corresponding principle" by Criss and Cobble¹⁷

Ion	$\overline{C_p^0} _{T_1}^T$, J mol ⁻¹ K ⁻¹
OH^- (aq)	$(215.01 - 0.72104T)/\ln(T/T_1)$
$Fe(OH)_3^-$ (aq)	$(328.85 - 1.1028T)/\ln(T/T_1)$
$Fe(OH)_4^-$ (aq)	$(345.27 - 1.158T)/\ln(T/T_1)$
FeO_4^{2-} (aq)	$(341.97 - 1.147T)/\ln(T/T_1)$

equilibrium constant of the reaction (1) is given by the equilibrium water activity at the given temperature:

$$\log K_{(1)} = -\Delta G_{(1)}^0 / 2.3RT = 4 \log a_{\text{H}_2\text{O}} . \quad (16)$$

From the dependence of water activity in KOH solutions on m_{KOH} and temperature⁸

$$\begin{aligned} \log a_{\text{H}_2\text{O}} = & -0.02255 m_{\text{KOH}} + 0.001434 m_{\text{KOH}}^2 + \\ & + (1.38 m_{\text{KOH}} - 0.9254 m_{\text{KOH}}^2)/T \end{aligned} \quad (17)$$

the associated KOH molality, at which all three solid phases may coexist with KOH solution at the given temperature, can be calculated on the basis of relations (16) and (17) for $T < T_c$:

$$\begin{aligned} m_{\text{KOH},r} = & \{0.02255 - 1.38/T - [(0.02255 - 1.38/T)^2 + \\ & + \log K_{(1)}(0.001434 - 0.9254/T)]^{0.5}\} / (0.002868 - 1.8508/T) . \end{aligned} \quad (18)$$

The values of $\log K_{(1)}$, $a_{\text{H}_2\text{O},r}$ and the associated KOH molality, $m_{\text{KOH},r}$, are given in Table IV for some temperatures. The regions of existence of individual solid phase as a function of KOH molality and temperature are shown in Fig. 1. With increasing KOH molality the point of transition of $\text{Fe}(\text{OH})_2$ to Fe_3O_4 and Fe is shifted to lower temperatures. Thus, $\text{Fe}(\text{OH})_2$ cannot exist at $m_{\text{KOH}} > 6.346 \text{ mol kg}^{-1}$ at 25°C . In accordance with these conclusions $E_{(3)}^0 = E_{(5)}^0$ at $T_c = 336.25 \text{ K}$ (63.1°C). Below this temperature $E_{(3)}^0 < E_{(5)}^0$ and above this temperature $E_{(3)}^0 > E_{(5)}^0$. This means that at $t < 63.1^\circ\text{C}$, solid

TABLE IV
Calculated values of individual parameters for chemical reactions (1), (2) and (9) for the temperature range of $25\text{--}125^\circ\text{C}$

Reaction parameters	$t, {}^\circ\text{C}$				
	25	50	75	100	125
(1) $\Delta G^0, \text{J mol}^{-1}$	4 133	1 477.6	-1 389.5	-4 454	-7 704
$\log K$	-0.72410	-0.23884	0.20848	0.62349	1.01076
$a_{\text{H}_2\text{O},r}$	0.6591	0.8715	(1.1275)	(1.4318)	(1.7893)
$m_{\text{KOH},r}$	6.3473	2.6974	-	-	-
(2) $\Delta G^0, \text{J mol}^{-1}$	34 313	35 722	37 571	39 857	42 578
(9) $\Delta G^0, \text{J mol}^{-1}$	84 998	91 326	98 948	107 828	117 941

Fe(OH)_2 is the thermodynamically stable product of iron corrosion in pure water whereas at $t > 61.3$ °C Fe_3O_4 is formed. With increasing KOH molality, however, the temperature limit for the formation of Fe_3O_4 instead of Fe(OH)_2 is shifted towards lower temperatures, as can be seen from Fig. 1. The equilibrium cell reactions potential corresponding to reactions (3) and (5) is given by expressions

$$E_{(3)} = E_{(3)}^0 - (2.3RT/2F) \log (a_{\text{H}_2\text{O}}^2/a_{\text{H}_2}) \quad (19)$$

and

$$E_{(5)} = E_{(5)}^0 - (2.3RT/2F) \log (a_{\text{H}_2\text{O}}/a_{\text{H}_2}) , \quad (20)$$

where the dependence of both water and hydrogen activities on the reaction conditions has to be taken into consideration. The gaseous activity at hydrogen reference electrode is given by the relation

$$a_{\text{H}_2} = (P - p_{\text{H}_2\text{O}}) \gamma_{\text{H}_2} , \quad (21)$$

where $p_{\text{H}_2\text{O}}$ represents the equilibrium pressure of water vapour over the KOH solution at m_{KOH} and given temperature, and γ_{H_2} is the fugacity coefficient of hydrogen at given total pressure P and temperature. The water vapour equilibrium pressure for $m_{\text{KOH}} =$

TABLE V

Calculated values of E^0 for electrochemical reactions (3)–(8) and (10)–(14) for the temperature range of 25–125 °C

Reaction	E^0 , V				
	25 °C	50 °C	75 °C	100 °C	125 °C
(3)	-0.09178	-0.09812	-0.10389	-0.10914	-0.11823
(4)	0.08604	0.08691	0.09063	0.09713	0.10636
(5)	-0.08643	-0.09622	-0.10570	-0.11492	-0.12390
(6)	-0.07036	-0.09047	-0.11110	-0.13223	-0.15384
(7)	-0.60381	-0.64569	-0.69492	-0.75146	-0.81528
(8)	-0.33860	-0.36778	-0.40172	-0.44040	-0.48381
(10)	0.10187	0.10533	0.11046	0.11718	0.12541
(11)	0.19182	0.18809	0.18476	0.18181	0.17922
(12)	1.51324	1.60735	1.72121	1.85444	2.00678
(13)	1.66743	1.65204	1.63633	1.62028	1.60386
(14)	1.52060	1.49514	1.46889	1.44190	1.41422

2–18 mol kg⁻¹ and the temperature range of 0–200 °C can be taken from ref.⁸, with $m_{\text{KOH}} = m$ and pressure in bar:

$$\begin{aligned} \log p_{\text{H}_2\text{O}} = & -0.01508m - 0.001679m^2 + 2.25887 \cdot 10^{-5}m^3 + (1 - \\ & - 0.001206m + 5.6024 \cdot 10^{-4}m^2 - 7.8228 \cdot 10^{-6}m^3)(35.44623 - \\ & - 3343.93/T - 10.9 \log T + 0.0041645T) . \end{aligned} \quad (22)$$

The expression for the fugacity coefficient γ_{H_2} in the same temperature range and the pressure from 1 to 200 bar can be taken from ref.¹⁸. For the temperature range of 0–150 °C and $P = 1.0$ –50 bar it can be substituted by a simple relation

$$\log \gamma_{\text{H}_2} = (3.77 \cdot 10^{-4} - 4.23 \cdot 10^{-7}T)P . \quad (23)$$

In order to evaluate correctly equilibrium conditions for reactions with the participation of soluble ionic substances it is necessary to know the activity coefficients of these ions under real reaction conditions. Unfortunately, this prerequisite is not sufficiently fulfilled for concentrated multicomponent solutions of the system under study both at room and at elevated temperatures. Therefore, in the case of reactions (2), (4), (7), (8), (9), (10) and (12), where equal number of moles of anions carrying equal charge appears on both sides of reaction equations, the ratio of the activity coefficients of these anions can be regarded as equal to 1.0 since a common solution with the same ionic strength is involved in the equilibrium state. Furthermore, due to the fact that $m_{\text{Fe(OH)}_3^-} \ll m_{\text{OH}^-}$ as well as $m_{\text{Fe(OH)}_4^-} \ll m_{\text{OH}^-}$, it may be assumed that $m_{\text{OH}^-} = m_{\text{KOH}}$.

The equilibrium molality of ions Fe(OH)_3^- and Fe(OH)_4^- was calculated by solving relations for equilibrium constants of chemical reactions (2) and (9) and Nernst equations for electrochemical reactions (4), (7), (8), (10) and (12), for the given reaction

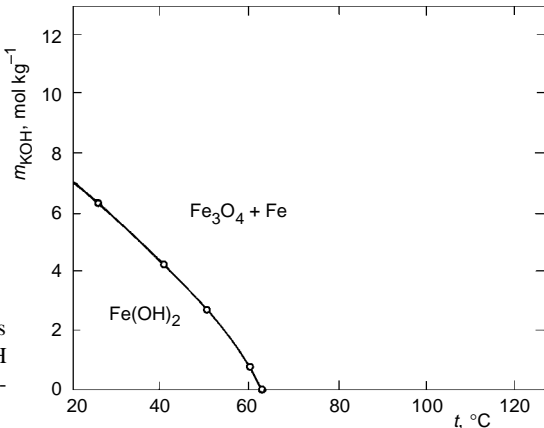


FIG. 1
Thermodynamic stability regions of solids Fe(OH)_2 , Fe_3O_4 and Fe in aqueous KOH solutions in dependence on the KOH molality and temperature

conditions. For example, the potential-independent equilibrium molality $m_{\text{Fe(OH)}_3^{3-}}$ was calculated using the relation

$$\log m_{\text{Fe(OH)}_3^{3-}} = -\Delta G_{(2)}^0/2.3RT + \log m_{\text{KOH}} \quad (24)$$

which holds for the quite narrow region of existence of solid Fe(OH)_2 (see Figs 2 and 3 for 25 °C). Below the equilibrium potential of cell reaction (3), the equilibrium molality of Fe(OH)_3^{3-} is governed by the relation (P and $p_{\text{H}_2\text{O}}$ is to insert in bar)

$$\begin{aligned} \log m_{\text{Fe(OH)}_3^{3-}} = & 2F(E_r - E_{(4)}^0)/2.3RT + 2 \log a_{\text{H}_2\text{O}} + \\ & + \log m_{\text{KOH}} - \log (P - p_{\text{H}_2\text{O}}) - \log \gamma_{\text{H}_2} . \end{aligned} \quad (25)$$

The calculated equilibrium data of $\log m_{\text{Fe(OH)}_3^{3-}}$ and $\log m_{\text{Fe(OH)}_4^{4-}}$ are fitted by dotted lines to the numerical logarithm values in Figs 2–5.

The molar ratio of Fe(II)/Fe(III) anions in saturated KOH solutions was calculated from the relation

$$\begin{aligned} \log (m_{\text{Fe(OH)}_3^{3-}}/m_{\text{Fe(OH)}_4^{4-}}) = A = & F(E_{(10)}^0 - E_r)/2.3RT - \log a_{\text{H}_2\text{O}} + \\ & + 0.5 \log (P - p_{\text{H}_2\text{O}}) + 0.5 \log \gamma_{\text{H}_2} . \end{aligned} \quad (26)$$

At positive potentials $E_r \geq 1.5$ V (RHE), when oxygen evolution from aqueous KOH solutions represents the main anodic process, solid Fe_2O_3 can be oxidized to soluble

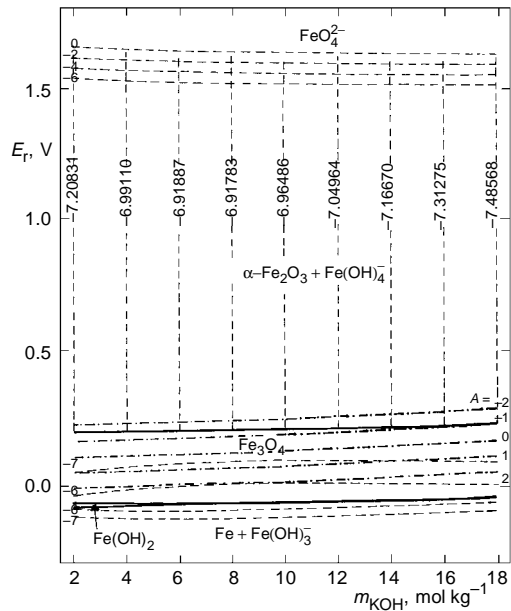


FIG. 2
 E_r - m_{KOH} diagram for iron at 25 °C and total pressure 1 bar (meaning of individual lines see in text)

FeO_4^{2-} . However, an exact evaluation of reactions (13) and (14) is more complicated since only less reliable thermodynamic standard data of $\text{FeO}_4^{2-}(\text{aq})$ are available¹⁵ and anions with different charges appear on both sides of reaction equations. Based on the assumption of low solubility (0.00909 M K_2FeO_4) in 14.58 M KOH at 20 °C (ref.¹⁹), $\gamma_{\text{OH}^-} = \gamma_{\pm\text{KOH}}$, $\gamma_{\text{FeO}_4^{2-}} = \gamma_{\pm\text{K}_2\text{FeO}_4}^2$ and $m_{\text{FeO}_4^{2-}} \ll m_{\text{OH}^-}$, i.e. $m_{\text{OH}^-} = m_{\text{KOH}}$, the following relation is obtained for the equilibrium molality $m_{\text{FeO}_4^{2-}}$ upon oxidation of Fe_2O_3 according to reaction (14):

$$\log m_{\text{FeO}_4^{2-}} = 3F(E_r - E_{(14)}^0)/2.3RT + 2 \log m_{\text{KOH}} + 0.5 \log a_{\text{H}_2\text{O}} - 1.5 \log (P - p_{\text{H}_2\text{O}}) - 1.5 \log \gamma_{\text{H}_2} + \log (\gamma_{\pm\text{KOH}}/\gamma_{\pm\text{K}_2\text{FeO}_4}) . \quad (27)$$

Since there is a lack of literature data for the dependence of mean activity coefficient ratio on the composition of solution and its temperature, we have assumed that this ratio is close to 1 so that $\log (\gamma_{\pm\text{KOH}}/\gamma_{\pm\text{K}_2\text{FeO}_4}) \approx 0$ and may thus be neglected in Eq. (27). The calculated values of $\log m_{\text{FeO}_4^{2-}}$ are plotted in Figs 2, 4 and 5 by dotted lines in the potential region of $E_r \geq 1.5$ V (RHE). However, it must be added that the ferrate ions are thermodynamically unstable since they may decompose spontaneously in alkaline solutions to solid Fe_2O_3 and/or $\text{Fe}(\text{OH})_4^-$ releasing gaseous oxygen according to

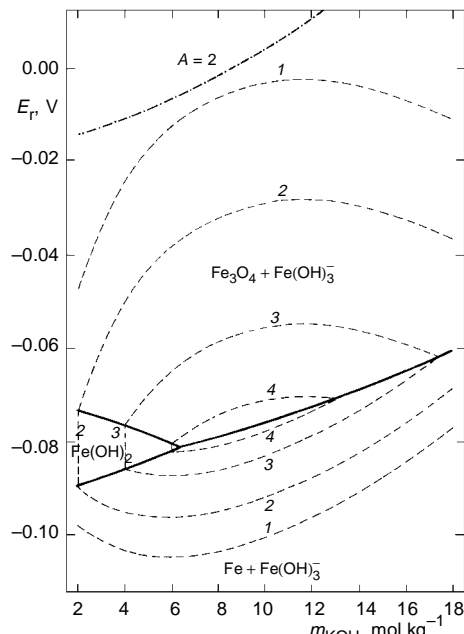
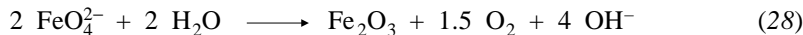


FIG. 3

E_r – m_{KOH} diagram for iron in the potential range –0.11 to +0.01 V (RHE) at 25 °C and total pressure 1 bar; $\log m_{\text{Fe}(\text{OH})_3^-}$ (m in mol kg^{-1}): –6.0 (1), –5.71 (2), –5.41 (3) and –5.233 (4)

and



The decomposition of FeO_4^{2-} ions in strongly alkaline solutions investigated in detail in refs^{20,21}, was not considered in the present study. Therefore, the course of the calculated equilibrium molality of FeO_4^{2-} ions in Figs 2, 4 and 5 should be taken as tentative.

RESULTS AND DISCUSSION

The results of the thermodynamic calculations for the system under study are shown in Figs 2 and 3 for 25 °C and total pressure $P = 1$ bar, in Fig. 4 for 100 °C and total pressure 10 bar and in Fig. 5 for 125 °C and total pressure of 30 bar. However, on the basis of given relations for $a_{\text{H}_2\text{O}}$, $p_{\text{H}_2\text{O}}$ and γ_{H_2} , the calculations can be performed in the range of $m_{\text{KOH}} = 2\text{--}18 \text{ mol kg}^{-1}$ for any reaction conditions in the range of 0–200 °C and pressure range of 1–50 bar (using Eq. (23)) or up to 200 bar (using Eq. (40) from ref.¹⁸ for fugacity coefficient γ_{H_2}). The RHE-scale of equilibrium potentials is experimentally easily to realize and completely free of any liquid junction potential; this represents a significant advantage in comparison to the classical Pourbaix diagrams.

Very interesting results not achievable using the usual form of E_r –pH diagrams after Pourbaix¹ were obtained for conditions of the spontaneous iron corrosion in KOH solu-

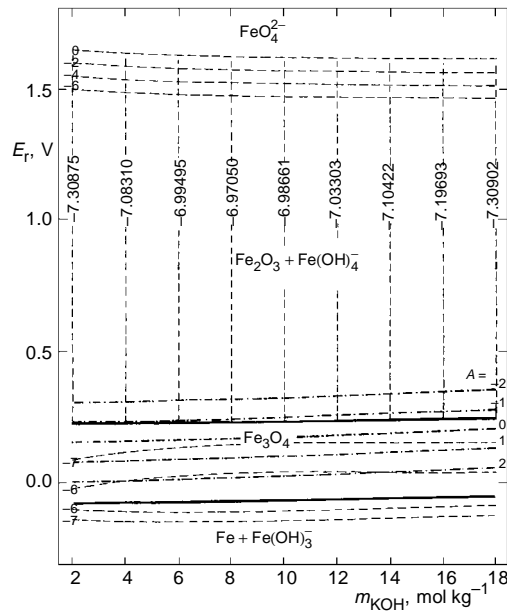


FIG. 4
 E_r – m_{KOH} diagram for iron at 100 °C and total pressure 10 bar (meaning of individual lines see in text)

tions when the true water activity was taken into account. At potentials from about -0.09 to -0.05 V (RHE) metallic iron is spontaneously corroded at $m_{\text{KOH}} = 2$ – 6.3 mol kg $^{-1}$ at the room temperature first to solid Fe(OH)_2 and at $m_{\text{KOH}} > 6.35$ mol kg $^{-1}$ directly to Fe_3O_4 , releasing gaseous hydrogen. The region of existence of solid Fe(OH)_2 is very narrow and wedge-shaped, as can be seen in the enlarged scale in Fig. 3. The stability limit of metallic iron is shifted towards more positive potentials with increasing KOH molality. On the contrary, equilibrium potential of Fe(OH)_2 oxidation to Fe_3O_4 is shifted towards more negative values with increasing KOH molality. Dotted lines in the lower potential range show the constant values of the equilibrium molalities of Fe(OH)_3^- as a function of m_{KOH} and electrode potential for the given temperature and total pressure. In the region of existence of solid Fe(OH)_2 they run vertically since in this region they are potential-independent. At the triple point with critical molality $m_{\text{KOH}} = 6.347$ mol kg $^{-1}$ and critical potential $E_{\text{cr}} = -0.0813$ V (RHE) at 25°C , when metallic iron can coexist with solid Fe(OH)_2 and magnetite, Fe_3O_4 , the equilibrium molality of Fe(OH)_3^- is given by $\log m_{\text{Fe(OH)}_3^-} = -5.209$. This value also represents the highest equilibrium molality at 25°C in the entire range of potentials and KOH molality considered.

In the region of coexistence of solid magnetite, apart from Fe(OH)_3^- ions, Fe(OH)_4^- anions may also occur to an increasing extent with increasing electrode potential in KOH solutions. The decadic logarithm of molar ratio of both anions, given as A (see Eq. (27)), is plotted in Figs 2–5 by dash-dotted lines. As can be seen, the fraction of Fe(OH)_4^- at potentials close to 0.0 V (RHE) for all reaction conditions is still fairly low

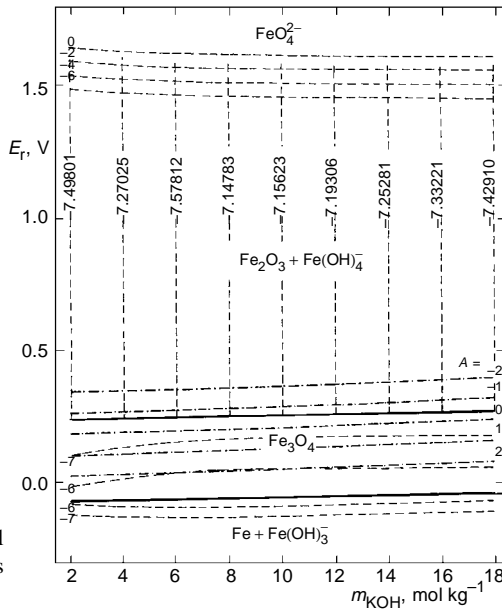


FIG. 5
 E_r - m_{KOH} diagram for iron at 125°C and total pressure 30 bar (meaning of individual lines see in text)

and amounts to about one hundredth of the equilibrium molality of Fe(OH)_3^- ions. At potentials of the oxidation of magnetite to haematite, $\alpha\text{-Fe}_2\text{O}_3$, the fraction of Fe(OH)_3^- ions always remains perceptible and actually increases with rising temperature, although Fe(OH)_4^- ions are already in the majority in the solution (see the shift of the curves for $A = -1$ and -2 in Figs 2, 4 and 5). Nevertheless, the total quantity of dissolved Fe(II) and Fe(III) ions remains very low. This is also demonstrated by the potential-independent equilibrium molality of Fe(OH)_4^- in the entire region of existence of $\alpha\text{-Fe}_2\text{O}_3$, which for $m_{\text{KOH}} = 2\text{--}18 \text{ mol kg}^{-1}$ is in the order of 10^{-7} to $10^{-8} \text{ mol kg}^{-1}$ at 25°C and actually decreases again with rising temperature after reaching the solubility maximum at 8 mol kg^{-1} of *ca* 8 mol kg^{-1} .

Above 1.45 to 1.5 V (RHE) , $\alpha\text{-Fe}_2\text{O}_3$ may be oxidized to soluble ferrate ions, FeO_4^{2-} . The results calculated for this potential range are, however, apparently less reliable than results obtained at more negative potentials where participation of lowervalency Fe substances is involved. There is a clear discrepancy between the standard data for $\text{FeO}_4^{2-}(\text{aq})$ after Wood¹⁵ (see Table I) and $\Delta H_f^0(\text{FeO}_4^{2-},\text{aq}) = -432.44 \text{ kJ mol}^{-1}$ which follows from $\Delta H_f^0(\text{K}_2\text{FeO}_4,\text{aq}) = -973.2 \text{ kJ mol}^{-1}$ and $\Delta H_f^0(\text{K}^+,\text{aq}) = -252.38 \text{ kJ mol}^{-1}$ at 25°C according to ref.¹³. The value for $\Delta G_f^0(\text{FeO}_4^{2-},\text{aq}) = -467.29 \text{ kJ mol}^{-1}$ at 25°C used by Pourbaix¹ (labelled by him with a question mark) displays even greater discrepancy with Wood's data. With respect to the solubility of K_2FeO_4 , $0.009 \text{ M K}_2\text{FeO}_4$ in 14.58 M KOH at 20°C , it could be expected that the existence region of solid K_2FeO_4 probably extends at potentials above the curve for $\log m_{\text{FeO}_4^{2-}}$ close to -2 so that the curve for $m_{\text{FeO}_4^{2-}}$ seems questionable, at least at room temperature. Thus, there is a need for new, more reliable standard data for $\text{FeO}_4^{2-}(\text{aq})$ as well as for solid K_2FeO_4 or other alkali metal ferrates.

Nevertheless, it can be concluded that the presented results showed clearly that the values of water activity under real reaction conditions must be considered in gathering sufficiently reliable data on equilibrium conditions in the course of chemical and electrochemical reactions in metal– H_2O systems. The usual method of constructing E –pH diagrams according to Pourbaix¹ based on the simplified assumption of $a_{\text{H}_2\text{O}} = 1.0$ in the entire pH range from -2 to $+16$ can lead to incorrect results at real reaction conditions deviating more distinctly from those at which this assumption is sufficiently valid.

REFERENCES

1. Pourbaix M.: *Atlas d'Equilibres Electrochimiques a 25 °C*. Gauthier–Villars, Paris 1963; English translation NACE, Houston 1974.
2. Townsend H. E., Jr.: *Corros. Sci.* **10**, 343 (1970).
3. Ashworth V., Boden P. J.: *Corros. Sci.* **10**, 709 (1970).
4. Misawa T.: *Corros. Sci.* **13**, 659 (1973).
5. Biernat R. J., Robins R. G.: *Electrochim. Acta* **17**, 1261 (1972).
6. Silverman D. C.: *Corrosion-NACE* **38**, 453 (1982).
7. Huy Ha Le, Ghali E.: *J. Appl. Electrochem.* **23**, 72 (1993).

8. Balej J.: Int. J. Hydrog. Energy 10, 233 (1985).
9. Balej J., Divisek J.: Collect. Czech Chem. Commun. 62, 696 (1997).
10. Desai P. D.: J. Phys. Chem. Ref. Data 15, 967 (1986).
11. Chase M. W., Jr., Davies C. A., Downey J. R., Jr., Frurip D. J., McDonald R. A., Syverud A. N.: *JANAF Thermochemical Tables*, 3rd ed., Part I, II; J. Phys. Chem. Ref. Data 14, Suppl. 1 (1985).
12. Barin I.: *Thermochemical Data of Pure Substances*. VCH Verlagsgesellschaft, Weinheim 1989.
13. Wagman D. D., Evans W. N., Parker V. B., Schum R. H., Halow I., Bailey S. M., Churney K. L., Nuttall R. L.: *The NBS Tables of Chemical Thermodynamic Properties*, J. Phys. Chem. Ref. Data 11, Suppl. 2 (1982).
14. Heusler K. E., Lorenz W. J. in: *Standard Potentials in Aqueous Solutions* (A. J. Bard, R. Parsons and J. Jordan, Eds), p. 391. Dekker, New York 1985.
15. Wood R. H.: J. Am. Chem. Soc. 80, 2038 (1958).
16. Tremaine P. R., LeBlanc J. C.: J. Solution Chem. 9, 415 (1980).
17. Criss C. W., Cobble J. W.: J. Am. Chem. Soc. 86, 5385, 5390 (1964).
18. Balej J.: Int. J. Hydrog. Energy 10, 365 (1985).
19. Thomson G. W., Ockerman L. T., Schreyer J. M.: J. Am. Chem. Soc. 73, 1379 (1951).
20. Tousek J.: Collect. Czech Chem. Commun. 27, 908 (1962).
21. Beck F., Kraus R., Oberst M.: Electrochim. Acta 30, 173 (1985).